MODIFICATIONS AND CALIBRATION OF THE RAINFALL WEATHER GENERATOR FOR THE UPPER SANTA-CRUZ RIVER BASIN, ARIZONA

By

Eylon Shamir

HRC TECHNICAL NOTE NO. 94

HYDROLOGIC RESEARCH CENTER, SAN DIEGO, CALIFORNIA, USA

Supported by

Bureau of Reclamation Lower Colorado Region (Agreement # R16AC00024)

1 August 2017

TABLE OF CONTENTS

ABSTRACT

This report describes the development of the hourly precipitation Weather Generator (WG) for the Upper Santa Cruz River Basin, near the crossing of the international Mexico-U.S border. This WG was developed as a tool to assess the impact on the water resources of various natural and man-made changes in the basin. In addition, it was used to explore various water resources management and planning schemes in order to advise for a management scheme that best addresses water resources challenges. The WG was developed as a point process model that is based on the assumption that the distribution of independent storms has a distribution of storm arrival time that is also independent and can be represented by a Poisson process.

ACKNOWLEDGMENTS

Major funding for this project was provided by the Bureau of Reclamation (BoR), Science and Technology Grant Program under a cooperative agreement between the Hydrologic Research Center and the BoR Lower Colorado Region (Agreement # R16AC00024). The authors wish to thank the project manager Dr. Eve Halper, BoR Phoenix Area Office for her technical and managerial assistance. Thanks are extended to Dr. Nicholas Graham from HRC that patiently participated in numerous brainstorming sessions that assisted with the development of a few of the concepts presented in this report. The opinions expressed in this report are those of the author and do not reflect those of the funding agency or the individuals acknowledged.

This report should be cited as follows:

Shamir, E., 2017: Modification and calibration of the rainfall weather generator for the Upper Santa-Cruz River basin, Arizona *HRC Technical Note No. 94*. Hydrologic Research Center, San Diego, CA, 1 August 2017.

1. INTRODUCTION

This report describes the hourly precipitation weather generator (WG) that was developed for the Upper Santa Cruz River Basin (USCRB). The WG for this region was initially developed and used in Nelson (2010); Liu et al. (2012); Shamir et al. (2005, 2007a, b). The WG was later modified and recalibrated with additional 10 years of observed data (Eden et al. 2016; Shamir et al., 2015; Shamir 2014, 2017). In this report, we describe the latest version of the WG, which was further modified and tuned in July 2017.

The WG is a computer script that is capable of producing likely hourly precipitation time series for a point. A sufficiently large ensemble of synthetic likely precipitation scenarios represents the regional rainfall characteristics, natural variability and the uncertainty that is associated with the observed record.

In a previous analysis, the MM5 (PSU/NCAR mesoscale model MM5) was used to investigate the climatological spatial distribution of rainfall over the headwater to find a fairly uniform rainfall distribution over the drainage area (Shamir et al., 2007a). Therefore, the statistical characteristic of the observed rainfall time series near Nogales is assumed to represent well the rainfall characteristics of the entire basin drainage area.

The ability of the WG to produce likely-to-occur precipitation scenarios that are representative of the region in a probabilistic manner, makes it an appealing tool for water resources planning and management studies. In conjunction with hydrologic models that simulate the natural water system of interest, it can be used to assess the impact of a range of scenarios such as, changes in water demand, construction of various structures and projected future changes in the atmospheric input. In addition, the WG simulations can be used to identify best management practices that optimally accommodate numerous objectives that often may compete with each other.

2. Study Area

The Santa Cruz River is an ephemeral tributary of the Gila River, which is a branch of the Colorado River. From its headwater in the San Rafael Valley in Southern Arizona, the river flows southward into Mexico and bends northwards towards Arizona to cross again the international border near the city of Nogales. The river length in Mexico is about 60 km with short perennial sections. The sparsely populated drainage area consists of heavily grazed desert scrub with deciduous broad leaf forest in the higher elevations.

The summer (June-September) and winter (November-March) are the two main rainy seasons in this region. Spring (April-May) is mostly dry and fall (October) is dry with occasionally intense rainfall events that are triggered by remnants of Pacific tropical storms. Summer precipitation events from the North American Monsoon System consist of isolated convective cells of thunderstorms that cause intense short-lived and local afternoon rainfall showers that are distributed in space. Winter storms are commonly caused by large-scale low-pressure frontal systems that originate in the Pacific Ocean. The duration of the winter storms may extend for a few days with persistent rain over large areas.

The differences in the seasonal precipitation characteristics generate distinctly different streamflow responses. The winter storms produce a relatively slow rising streamflow followed by a prolonged recession (baseflow), while the summer flow events appear as a sudden and sharp rising streamflow followed by a relatively short period of baseflow (e.g. Shamir et al., 2007a). The seasonal precipitation differences between the summer and winter (1948-2017) and their large inter-annual variabilities are apparent in Figure 2.1. The differences in the hydrologic response characteristics and rainfall spatial variability of the two seasons contributes to the fact that, although the average summer precipitation is more than double of the average winter precipitation, both seasons have similar average streamflow (Shamir et al. 2015).

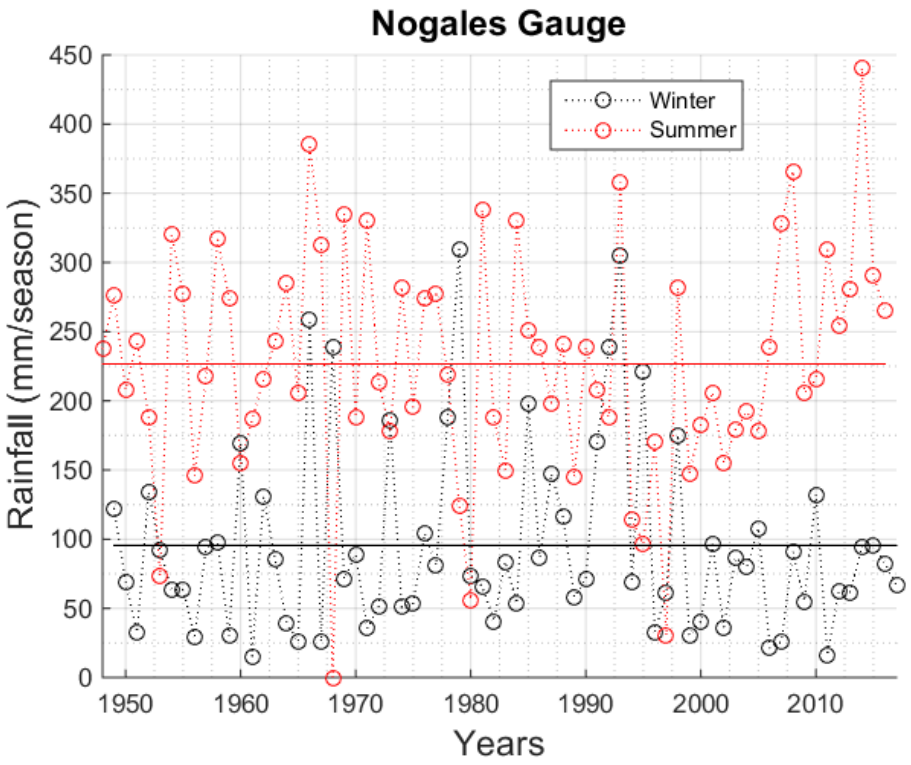

Figure 2.1 Total summer (red) and winter (black) precipitation in the USCRB. The straight lines indicate the average seasonal value (1948-2017)

3. DATA

Hourly precipitation time series were compiled for 7/1/1948 to 5/31/2017 from four quality-controlled rain gauge stations retrieved from the National Climatic Data Center, U.S. National Oceanic and Atmospheric Administration (Figure 3.1). The precipitation time series is based on a gauge located in the City of Nogales and missing periods were estimated from adjacent gauges using a linear regression derived from periods with overlapping records.

The monthly distribution of the diurnal hourly precipitation is shown in Figure 3.2. During the winter months, the occurrence of hourly precipitation is evenly distributed throughout the day. On the other hand, during the summer months (June-September)

the hourly precipitation events are concentrated in the afternoon and the evening while rarely occurring during the morning hours.

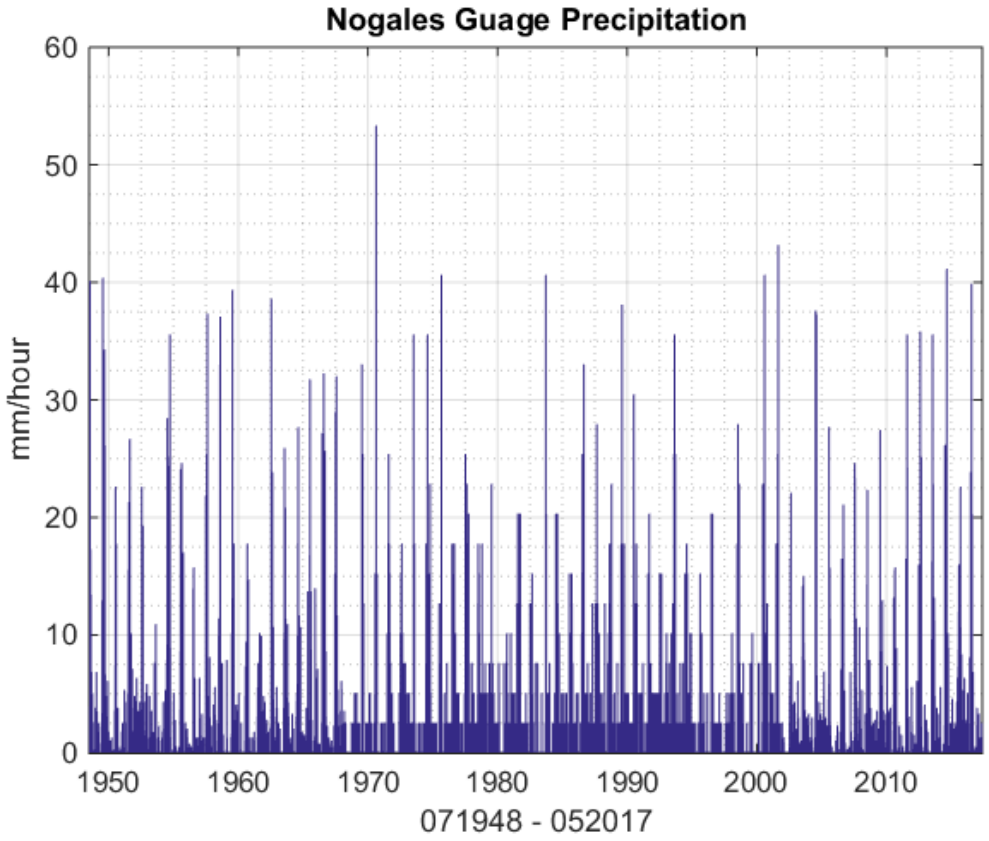

Figure 3.1: USCRB hourly precipitation time series (07/1948-05/2017)

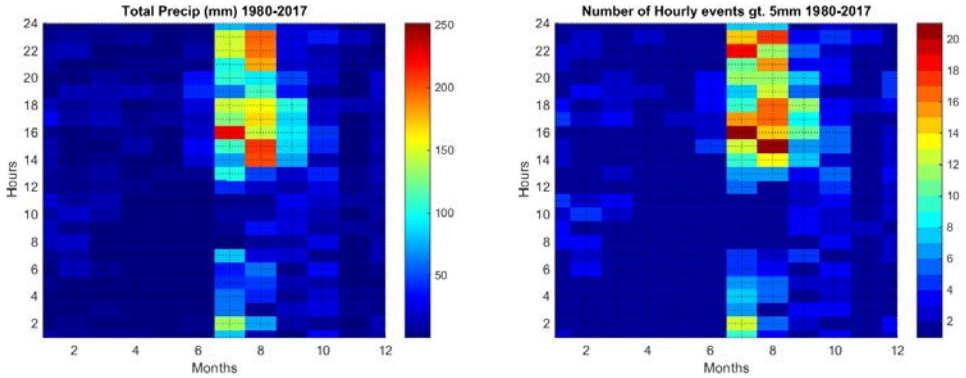

Figure 3.2: Monthly distribution of the diurnal precipitation, the total hourly precipitation (left) and number of hourly events that are greater than 5 mm (right).

To further illustrate the diurnal dynamic and differences between the seasons, see Figure 3.3. In this Figure the left two panels are histograms of the winter and summer portion of the wet days (greater than 10 and 20 mm/day for the winter and summer, respectively) that were contributed by the maximum hourly precipitation that occurred in these days. The right two panels are histograms of the number of wet hours that occurred during wet days.

The highest number of daily winter storms had hourly events that contributed about 20-30 percent of the daily precipitation and lasted about 5-7 hours. In the summer most wet days had hourly events that contributed more than 80% of the daily precipitation with most daily storms had 2 or 3 hourly occurrences. Thus, it can be seen that the diurnal distribution is a key feature of the temporal precipitation distribution in the region, and describing the precipitation scenarios at a daily time scale may smooth important seasonal differences that control the hydrologic response.

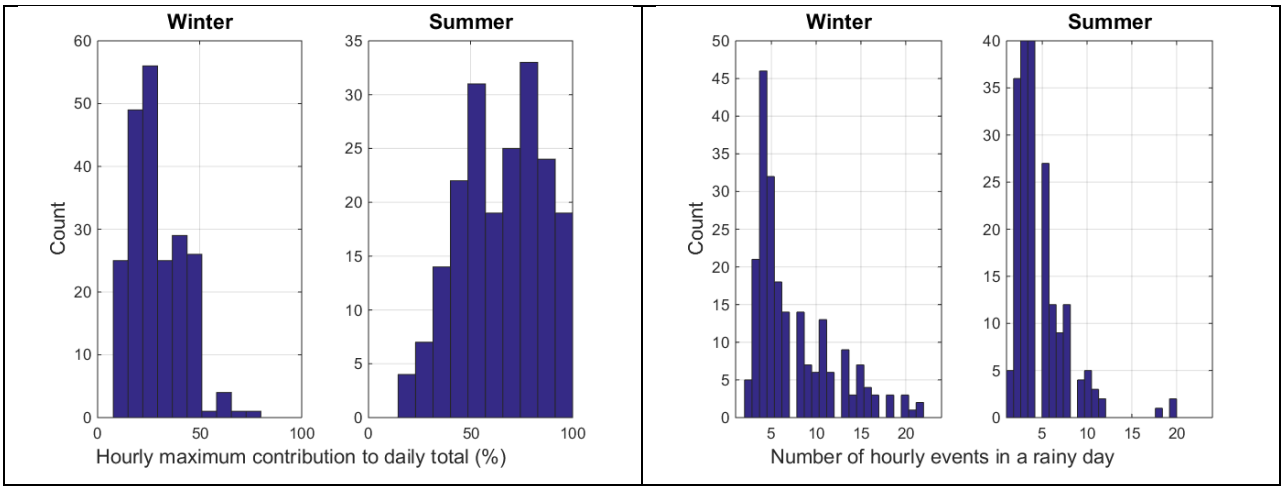

Figure 3.3: Left histograms are for the percent of the daily precipitation that is contributed by the maximum hourly precipitation event that occurred in these days. Right histograms are the number of hourly events that occurred during wet days.

The large diurnal variability of precipitation in the USCRB for summer requires the development of hourly WG. Although the development of hourly precipitation WG is essential in order to capture the diurnal characteristics, it is important to note the

following potential caveats. Compared with, for example, daily WG the development of hourly WG: 1) relies on a fewer observed records; 2) the existing observed records are often associated with larger error and more missing values; 3) the WG requires a more complex formulation with large number of model parameters to be optimized;

In summary, the analysis to follow is carried with the following major assumptions with regard to the observed record: 1) the time series represent the rainfall characteristics of the region; 2) The quality control procedures that were implemented were sufficient to resolve data quality issues and therefore we disregard uncertainties that are associated with the observed record; 3) the time series is stationary with no apparent trend; 4) year-to-year and season-to-season precipitation are independent and not associated with the previous season.

4. Precipitation Weather Generator Development

4.1 WG Conceptual Configuration

The point process WG that was developed in this study simulates hourly likely precipitation scenarios to represent four seasons: fall (October), winter (November-March), spring (April-May) and summer (June-September). Because of the large inter-annual precipitation variability in the winter and summer, these seasons are represented as three wetness categories (i.e., wet, normal and dry). The division of the wetness categories is based on terciles of the total seasonal precipitation (Figure 4.1). We note that although the wet seasons are associated with sea surface temperature of the Pacific Ocean (e.g. Shamir, 2017), a year-to-year and season-to-season dependency were not detected in the precipitation record. Therefore, we assume that the chance of a wetness category to occur is independent of the previous wetness category.

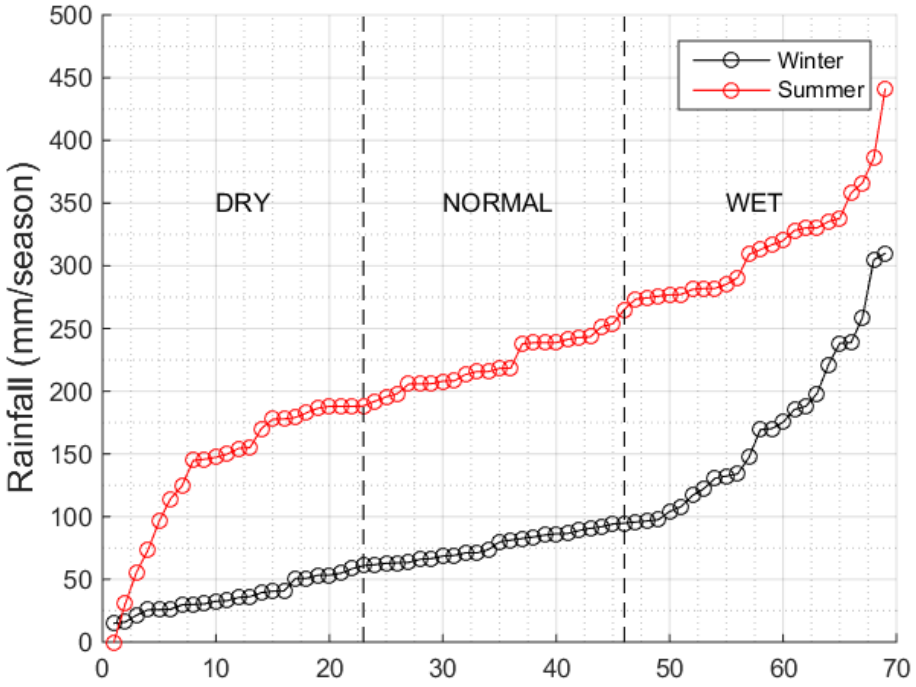

Figure 4.1: Sorted 1948-2017 precipitation total grouped by terciles to represent dry, normal and wet for summer (red) and winter (black) seasons.

For each of the wetness category of the winter and summer the WG produces likely scenarios following the sequence that is illustrated in Figure 4.2. The first step is to independently sample a wetness category. Next, the duration of the rainy season is defined by selecting the seasonal onset and offset. The first storm event of the season is sampled following the season onset and then the following steps are being carried repeatedly until the end of the season, which is determined by the selected offset. These repetitive steps consist of sampling for: a) the duration of the storm; b) chance of hourly precipitation to occur; c) the magnitude of hourly precipitation and; d) the dry duration until the next storm arrive.

For the spring and fall seasons which are commonly dry, the WG consists of sampling only for a chance for hourly precipitation to occur and the hourly precipitation magnitude. Although large precipitation events have occurred in October, there are no

sufficient data points to comprise a sample that can be used for analysis of storms inter-arrival time (IAT) and durations.

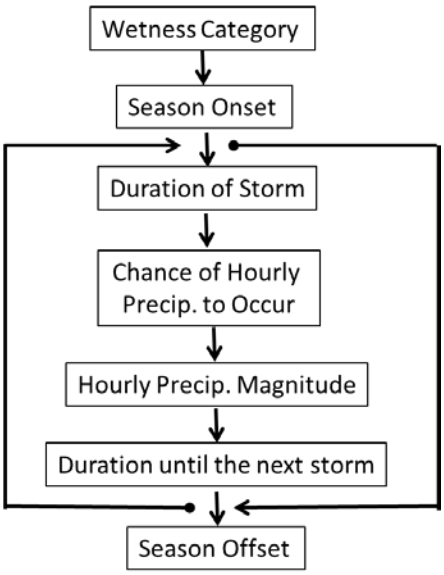

Figure 4.2: A schematic flowchart of the WG steps

The point process WG model developed herein is based on the assumption that precipitation storms tend to arrive in clusters as a response to transient synoptic scale atmospheric disturbances. Each transient synoptic event may produce a multiple hourly precipitation bursts with possible short dry spells in-between the precipitation bursts. The definition of a storm is a key requirement in order to derive a statistical sample of independent observed storms, which is the base for the WG development.

Two precipitation events which are spread by a dry spell of a several weeks are clearly the result of two different and independent synoptic systems. On the other hand, two precipitation events with a dry gap of a few minutes are likely to be from the same weather system and therefore dependent. Ideally, the derivation of a statistical sample of independent storms should be carried using a comprehensive analysis of atmospheric data to identify independent weather systems. An alternative empirical

method is to identify a critical period that, most of the time, separates the precipitation record into independent storm events.

The essential precipitation features that are required for hydrological applications are the time between storms, the duration of the storms and the storm precipitation depth (Eagleson, 1982). Arguably, these features are even more important in arid environment, in which the characteristics of the rainfall events are producing high variability flow events in ephemeral streams. An approach for identifying the critical period that may be attuned with hydrologic studies is to consider the precipitation time series in conjunction with streamflow or other watershed antecedent moisture indices (e.g. Istok et al. 1983). However, in the arid environment where many of the precipitation events do not generate runoff and the rainfall-streamflow relationships are highly non-linear, such an approach may not be adequate.

4.2 Poisson Process

In this study, we derive the independent sample of storms using the precipitation record exclusively. A review of the precipitation based empirical methods for selecting the critical duration is in Bonta and Rao, (1988). We selected a method that is based on the assumption that the arrival of independent storms conforms to a Poisson process. A Poisson process is a non-deterministic process where events occur continuously and independently of each other. The Poisson distribution is a discrete probability distribution that expresses the probability of a number of events occurring in a fixed period of time, given that these events occur with a known average rate and independently of the time since the last event. WGs with Poisson cluster processes at their core were shown to perform well across multiple time scales, range of rainfall characteristics and in many regions worldwide (e.g. Rodriguez-Iturbe et al.1987 and 1988).

Our definition of storms relies on the statistical assumption that the distribution of the storm inter-arrival time (IAT), that is, the duration from the end of a storm to the beginning of the next storm, constitutes a Poisson stochastic process. This implies that as in Poisson process, the distribution of storms inter-arrival time should conform to an exponential distribution (Restrepo-Posada and Eagleson, 1982). Accepting this

assumption it is feasible to identify a minimum inter-arrival time (MIAT) between storms (i.e. the minimum number of dry hours beyond which the occurrence of hourly rainfall marks the beginning of a new storm event) that yields a sample of independent distribution of storms IAT with a coefficient of variation of one, as in an exponential distribution. A schematic example of two independent storms that are separated by a critical duration is shown in Figure 4.3.

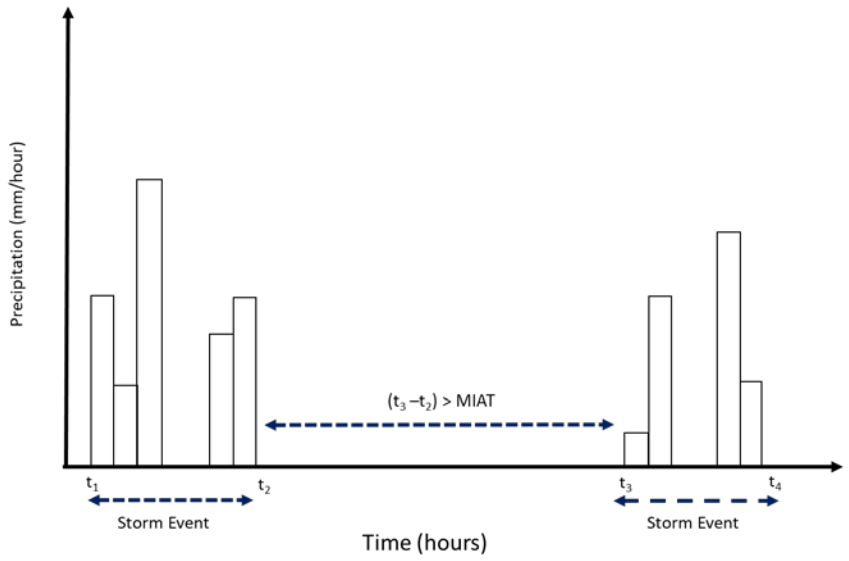

Figure 4.3: A schematic example of hourly precipitation pulses that demonstrates the empirical definition of independent storms.

In Figure 4.4, the coefficient of variation (CV) of the IAT distribution is plotted as a function of a range of MIAT values for the wetness categories of the winter and summer. It is important to assess the resulted sample of storms and evaluate whether most of the derived storms are with shorter duration than the selected MIAT. A Poisson process describes a random arrival of storm events with zero duration. The Poisson process assumption can be relaxed to include the case of storm events which have finite duration, by having storm events that are shorter than the IAT (Eagleson, 1982).

The MIAT values, in this study, were set to 24 and 12 hours for the winter and summer, respectively. The percent of storms (clusters) with duration that is less than the

MIAT is plotted as a function of the MIAT in Figure 4.5, For the summer, it can be seen that MIAT of 12 hours yields the highest number of clusters that are shorter than the MIAT (87%). In the winter the peak number of clusters that are shorter than the MIAT yield a CV that is smaller than 1. Therefore, we decided to use 24 hour for the winter which yield CV that is close to 1, although for about 20% of the storms the inter-arrival time may be longer than 24 hours. The numbers of storm events that were identified for the wetness categories are in Table 4.1.

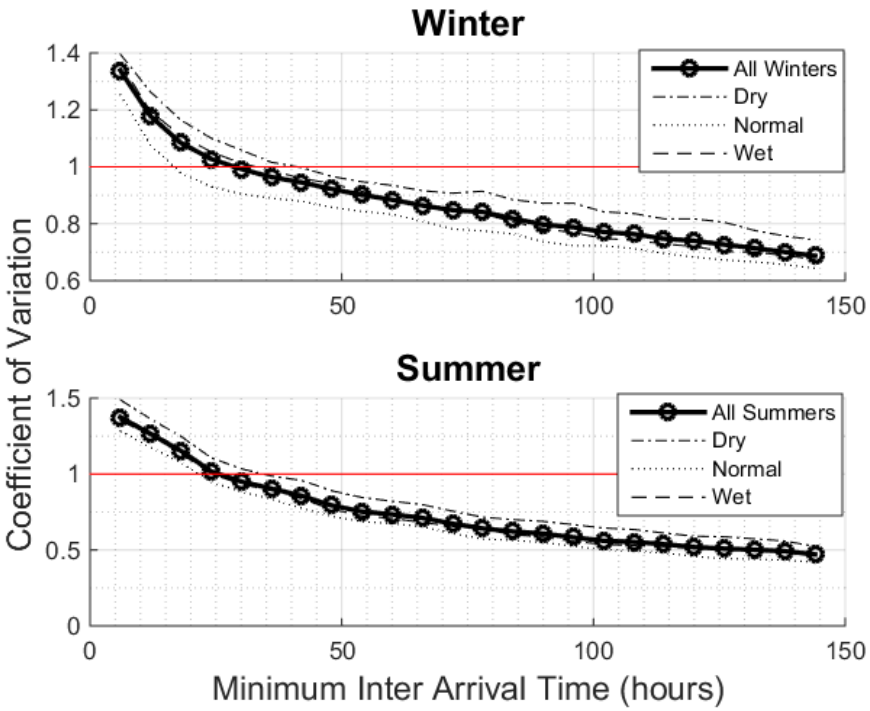

Figure 4.4: The Coefficient of Variation of the IAT distribution as a function of the MIAT for the winter (upper panel) and summer (lower panel).

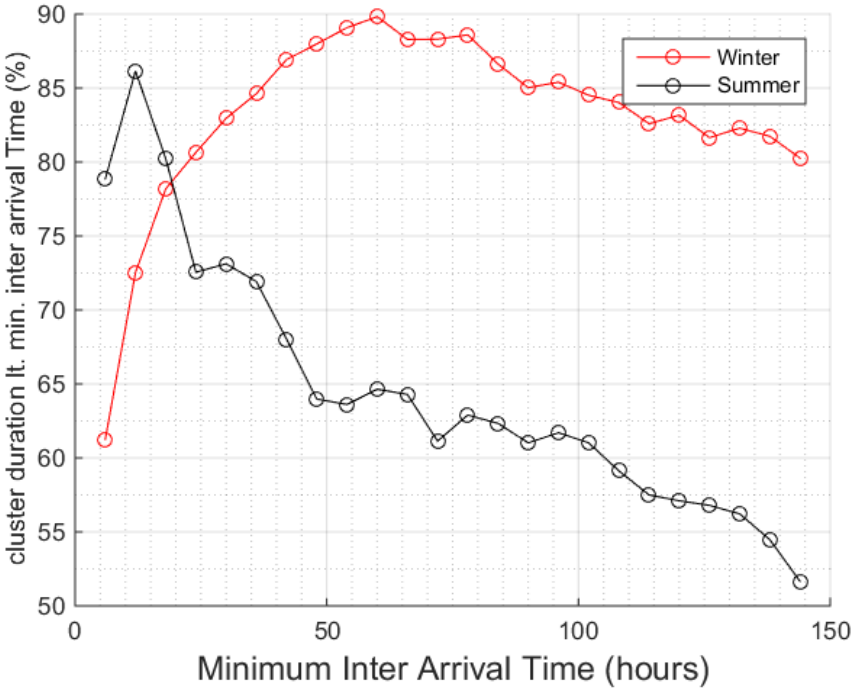

Figure 4.5: Percent of clusters with durations that are less than the MIAT

Table 4.1: Number of storm events 1948-2017

Winter			Summer		
Dry	Normal	Wet	Dry	Normal	Wet
173	250	353	446	629	716

4.3 Inter Arrival of Storms

The cumulative distributions of the winter and summer IAT of the three wetness categories are shown in Figure 4.6. The differences between the wetness categories within and between the seasons are clearly shown in this figure. As expected, the dry [wet] years have longer [shorter] IAT for both the winter and the summer. The time between storms during the winter extends longer than in the summer. For instance, the IAT at the 80 percentiles of the normal summer is 4.5 days, whereas for the normal winter it is about 19 days, which implies that the durations between winter storms is about four times longer than in the summer.

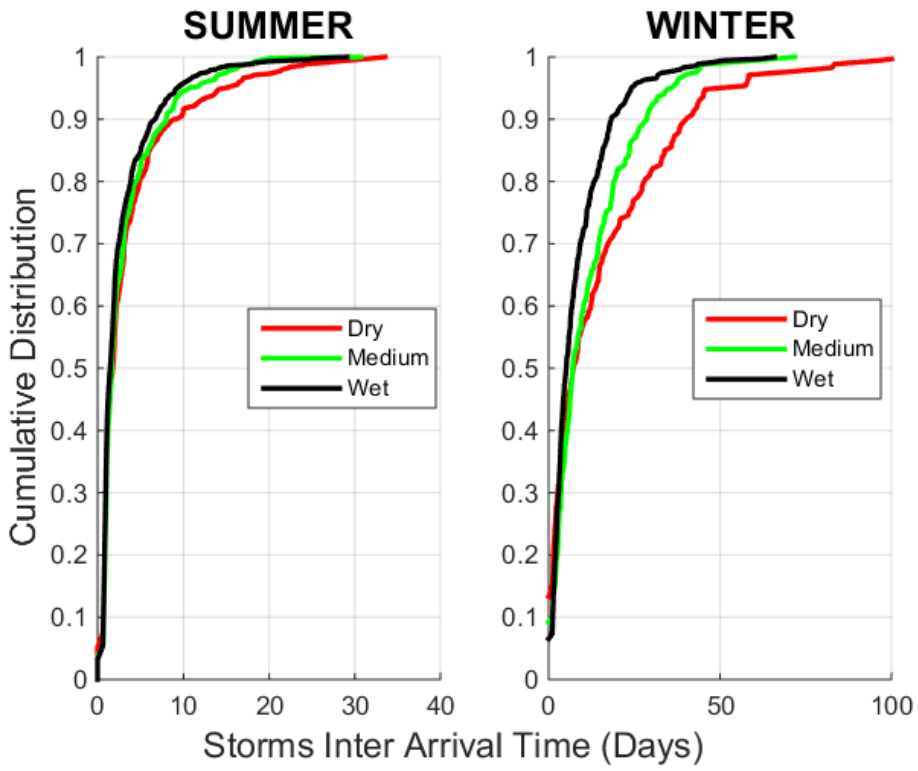

Figure 4.6: The cumulative distribution of the winter and summer storm inter-arrival time for the three wetness categories.

Following an exhaustive search among various statistical distributions, the samples of duration between storms (IAT) was fitted a Generalized Pareto (GP) distribution. The GP is a continuous distribution of exceedance over a pre-determined threshold. An exponential distribution is a special case of GP, in which the shape and threshold parameters equal zero. In our case, the MIAT is assigned as the GP threshold parameter and the scale and shape parameters were optimized to fit the observed record, using a maximum likelihood procedure.

The GP generalize form is:

$$G(\mathrm{y}:\sigma,\gamma) = \begin{cases} 1-\left(1+\gamma\frac{\mathrm{y}}{\sigma}\right)^{-1/\gamma}, & \gamma \neq 0 \\ 1-\exp\left(-\frac{y}{\sigma}\right), & \gamma = 0 \end{cases} \qquad (1)$$

where y is the series of exceedances over the threshold (x_i-u), x_i is a selected quantile, and σ and γ are referred to as the scale and shape parameters, respectively.

The fitted GP distribution and its 5% and 95% confidence intervals compared to the observed record are shown in Figure 4.7 and 4.8 for winter and summer, respectively. It is seen that the shape of the cumulative distribution of the dry winter category has the highest variance. In the WG algorithm, the IAT is sequentially sampled using two steps. First, a value is randomly sampled from the optimal set of parameters. Second, the IAT is sampled from a normal distribution $N(\mu, \sigma^2)$, in which the μ is assigned as the value sample in step one and the variance is estimated from the confidence intervals as follows, $\sigma^2 = \left(\frac{\mu - C.I_{95}}{2}\right)^2$.

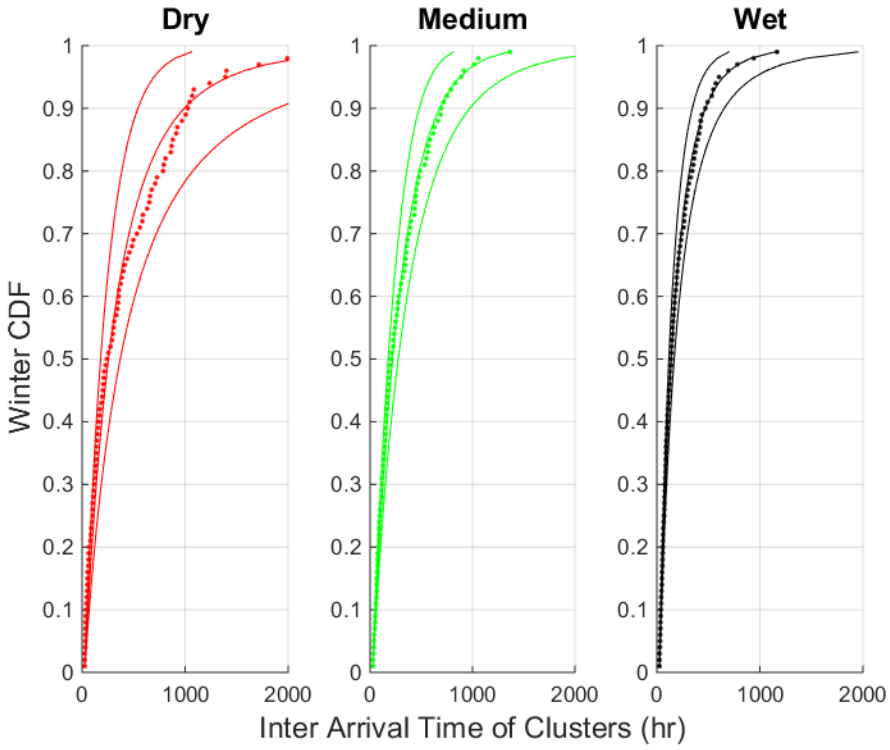

Figure 4.7: Cumulative distributions of the winter optimal GP fit with its 5 and 95% confidence intervals for the three wetness categories. Observed data are indicated as dots.

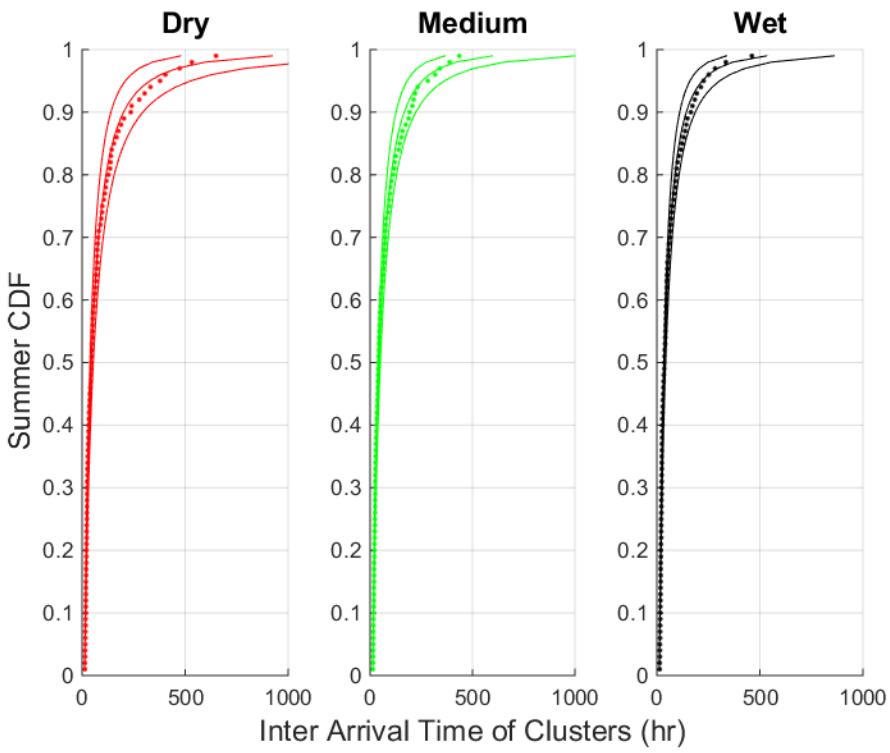

Figure 4.8: As Figure 4.4 but for summer

4.4 Seasonal Onset and Offset

The duration of the wet season in the USCRB is often a major factor that determines the wetness of the season. The duration is identified by both the first (onset) and the last (offset) storms of the season. The variability of the onset and offset and their association with the wetness categories are seen in Figure 4.9. It is shown for example that for both seasons the dry category was associated with shorter raining season as implies by larger onset and offset values. Note that the cumulative distribution in this plot is based on *only* 23 values that represent terciles. Because of this relatively small sample size, it is difficult to identify statistical distributions that well represent the onset and offset samples. In the WG, the onset and the offset are sampled from a normal distribution with the mean and standard deviation of the corresponding sampled CDF.

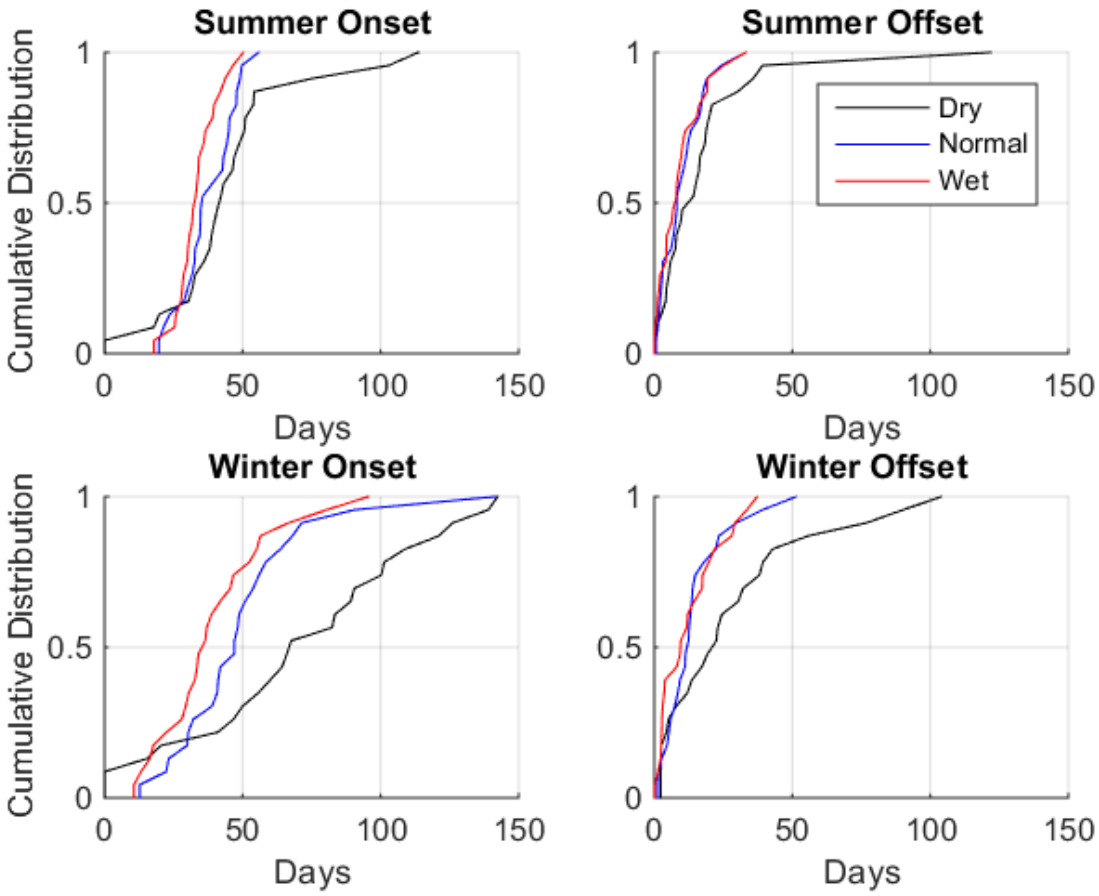

Figure 4.9: The cumulative distribution of the observed summer and winter precipitation onset and offset.

4.5 Storms Characteristics

The distribution of the duration of storms and the distribution of the magnitude of hourly precipitation bursts during the storms are shown in Figures 4.10 and 4.11, respectively. It is interesting to note that during the summer, for both the storm durations and the hourly magnitudes, the differences among the wetness categories appear to be small. In the winter, on the other hand, these differences are more visible but yet relatively small, with a possible exception being the cumulative frequencies of the very long durations.

Both these distributions were fitted with a Weibull distribution using a maximum likelihood procedure to derive the optimal and 5 and 95% confidence intervals. Although log normal distribution is often being used to describe the distribution of precipitation magnitude, in this study the Weibull found to better fit the observed dataset. A general expression for the two parameters of the Weibull PDF equation is as follows:

$$f(W) = \frac{\gamma}{\sigma}\left(\frac{y}{\sigma}\right)^{\gamma-1} e^{-\left(\frac{y}{\sigma}\right)^{\gamma}}, \qquad f(W) \geq 0, and\ y \geq 0 \qquad (2)$$

where y is the selected quantile and σ and γ are, as in Equation 1, the scale and shape parameters, respectively.

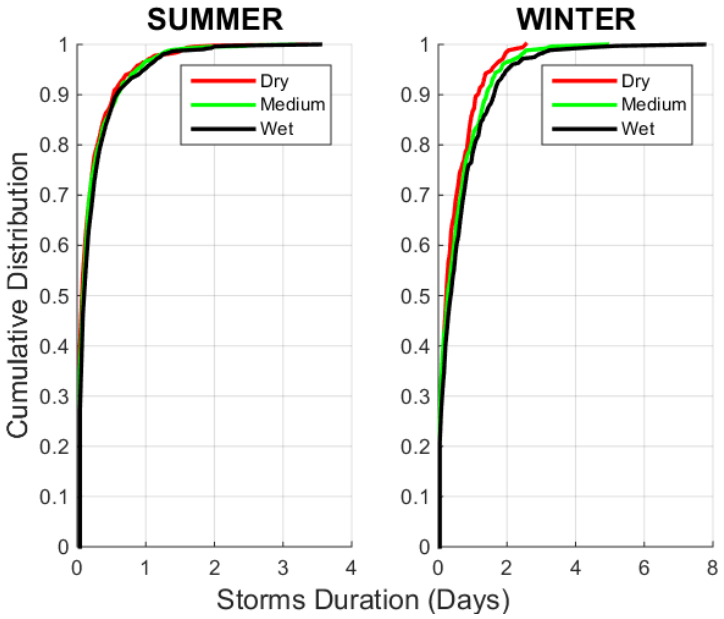

Figure 4.10: The cumulative distribution of the observed summer and winter storm duration

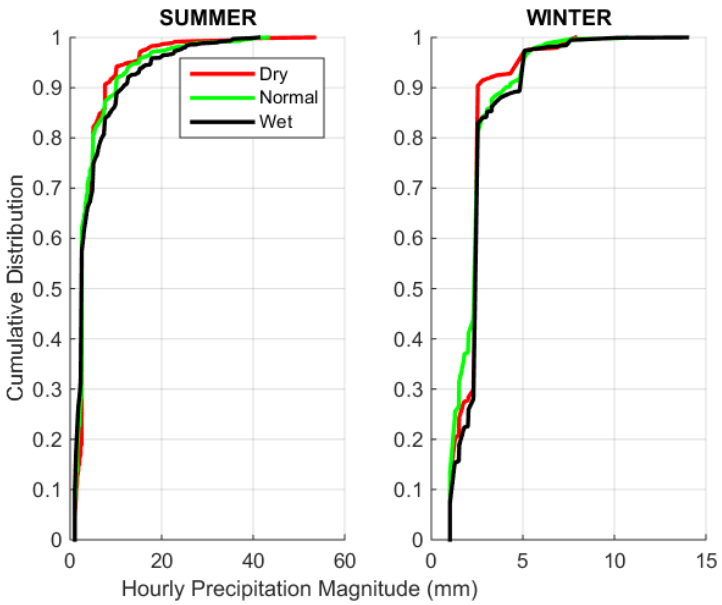

Figure 4.11: The cumulative distribution of the observed summer and winter hourly magnitude.

The distribution of the number of occurrences of hourly precipitation pulses during the storms is closely associated with the distribution of the storm duration (Figure 4.12). In the WG a storm always starts and ends with a precipitation event and may include hours with zero rainfall. As implies by this storm definition the chance for precipitation to occur in a short storm is higher than in a longer storm. We used the following scheme to sample the distribution of precipitation events within a storm.

In the WG we estimate the chance of hourly precipitation to occur for each storm using two steps: 1) Utilizing a linear regression to select the average number of hourly rainfall events as a function of the storm duration, 2) Sampling the number of hourly precipitation events randomly from a normal distribution with average that was estimated in the first step and variance which was calculated from the residuals of the regression. The chance of hourly precipitation to occur is applied independently for each hour as the ration between the estimated number of hourly precipitation and the storm duration. The regressions were derived for the winter and summer separately, without distinguishing among the three wetness categories (Figure 4.12).

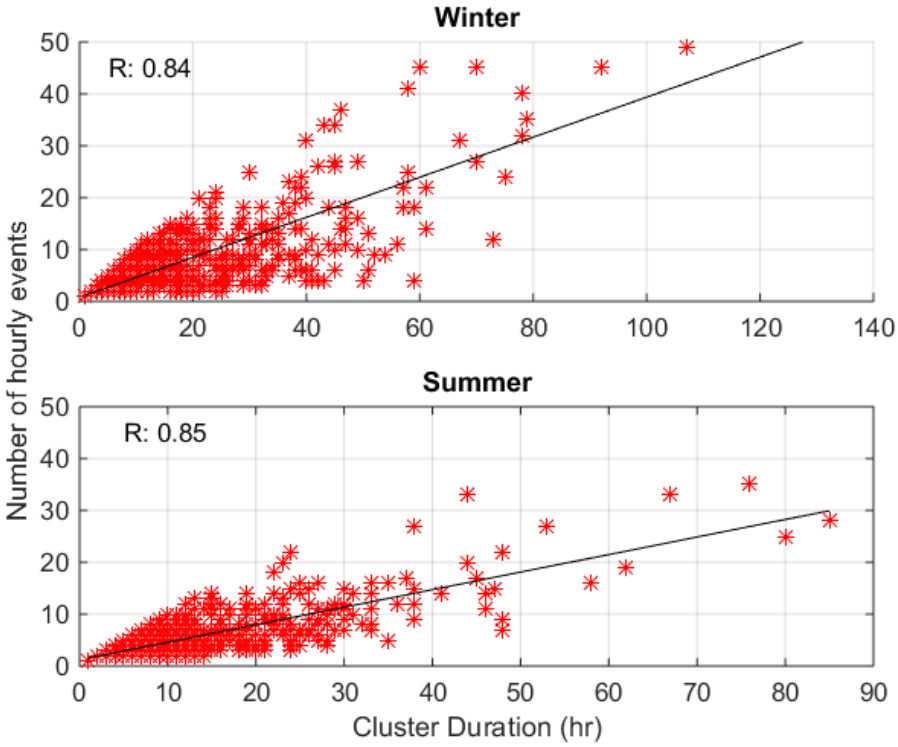

Figure 4.12: A scatter plot of the number of hourly events in a storm as a function of the storm duration.

5. WG Evaluation

In this section, we evaluate the WG simulations using an ensemble that includes 100 realizations, each realization has hourly precipitation for 69 years. The cumulative distribution of the total seasonal precipitation of the observed (red) and 100 realizations are shown in Figure 5.1. We note that the total seasonal value is a measure that was not accounted for in the derivation of the WG and therefore may be considered as an independent evaluation measure.

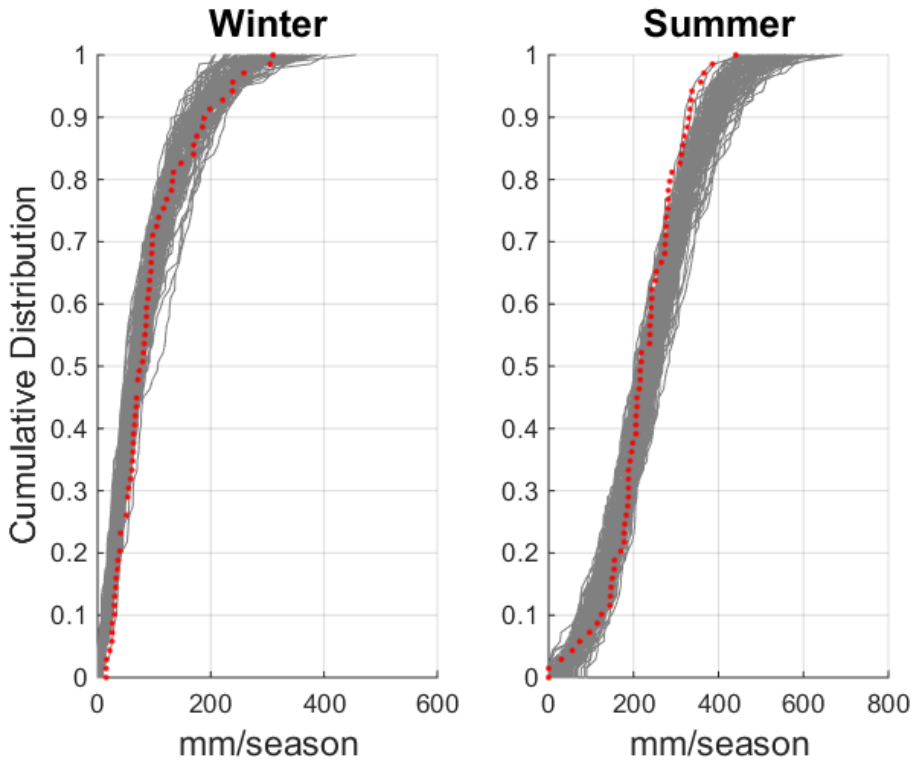

Figure 5.1: The cumulative inter annual distributions of the winter and summer total precipitation of the WG simulated ensemble (gray) and the observed record (red).

It is seen that the WG simulations capture the cumulative distribution of the observed fairly well. The distribution of the observation, for both winter and summer, has a shape that includes sharp changes, which can be difficult to capture. The winter simulations of the upper 80% are a bit dryer than the observed although the distribution of the very wet years embrace the observed record. On the other hand, the summer simulations of the upper 80% are wetter than the observations. Note that the WG was developed to describe the entire spectrum of precipitation and not necessary focus on the extreme values. Arguably, because the wet terciles in both seasons have the highest variability, in order to improve the WG performance of the extreme wet seasons the wet category should be further divided to include an additional category of very wet.

The model evaluation with respect to the number of seasonal hourly events is shown in Figure 5.2. It is seen that the observed inter-annual distribution is fairly well represented with under estimation of the winter's 90s percentiles.

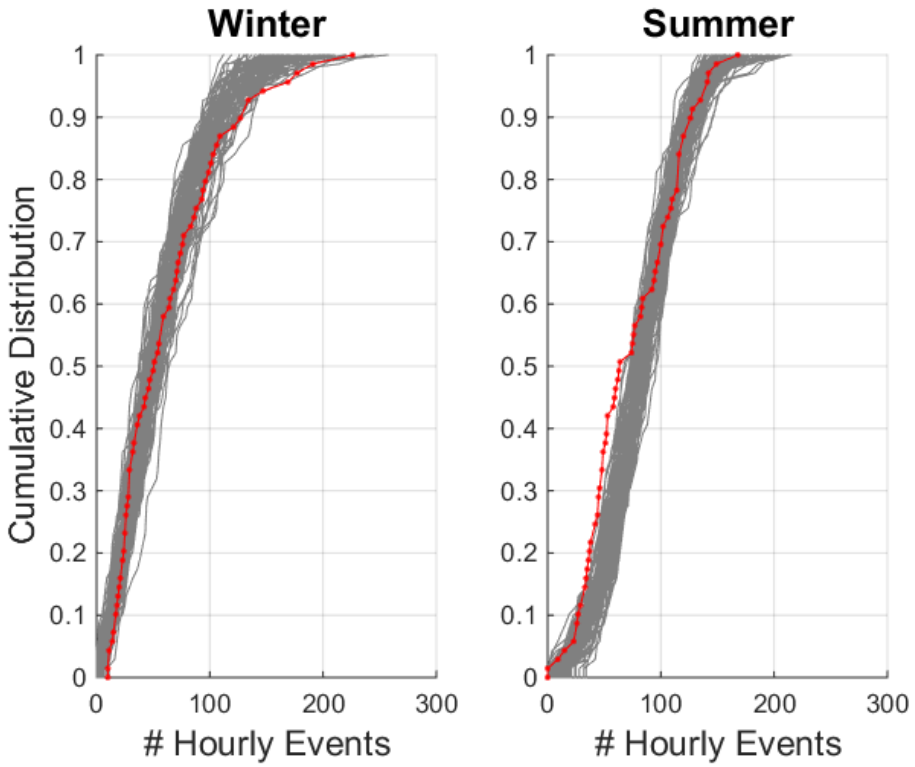

Figure 5.2: The cumulative inter-annual distributions of the winter and summer number of hourly events from the WG simulated ensemble (gray) and the observed record (red).

As far as we know, there is no formal method to evaluate the performance of an ensemble. The spread of the realizations of the ensemble should represent the uncertainty that is associated with the observed record. The width of the spread of the ensemble should neither be too wide or too narrow. An ensemble with realizations that have very similar CDFs, which will yield a narrow spread, does not describe the uncertainty and variability in the data. On the contrary, realizations with very different CDFs will fail to capture the unique characteristics of the data.

Herein we quantify the resulted spread of the ensemble by comparing it to the confidence intervals (CI) of the observed record. In order to derive these CI a Monte Carlo experiment of sampling with replacement a subset of the observed years was conducted. The sampling was carried 100 times for 40 sequentially reducing sample size (68-28 out of 69 years). The spread of the CI was identified for the 25, 50 and 75 percentiles of the CDF. In each sampled subset of years (100 repetitions), the percentiles of the values that were derived from the entire observed record at the 25, 50

and 75 percentiles were estimated. The CI for each sample size represents the distance between the 5 and the 95 percentiles of the 100 samples. The changes in the CI distances at the 25, 50 and 75 percentiles are shown in Figure 5.3 as a function of the subset sample size. The solid lines are moving averages with window size of 5 years of the actual values (dotted lines). It is seen, as expected that reducing sample size results in widening the spread of the CI.

The estimated spread of the ensemble at the 25, 50 and 75 percentiles of the CDF is indicated in Figure 5.3 by dashed horizontal lines with corresponding colors. The spread of the ensemble was estimated as follows. First, the median of the simulated values at the 25, 50 and 75 percentiles was estimated; second, the percentiles of these median values in the CDF of the 100 realizations were estimated; and third, the spread of the distribution for the three identified quantiles (25, 50 and 75 percent) was defined as the range between the 5th and 95th percentiles of the 100 estimates.

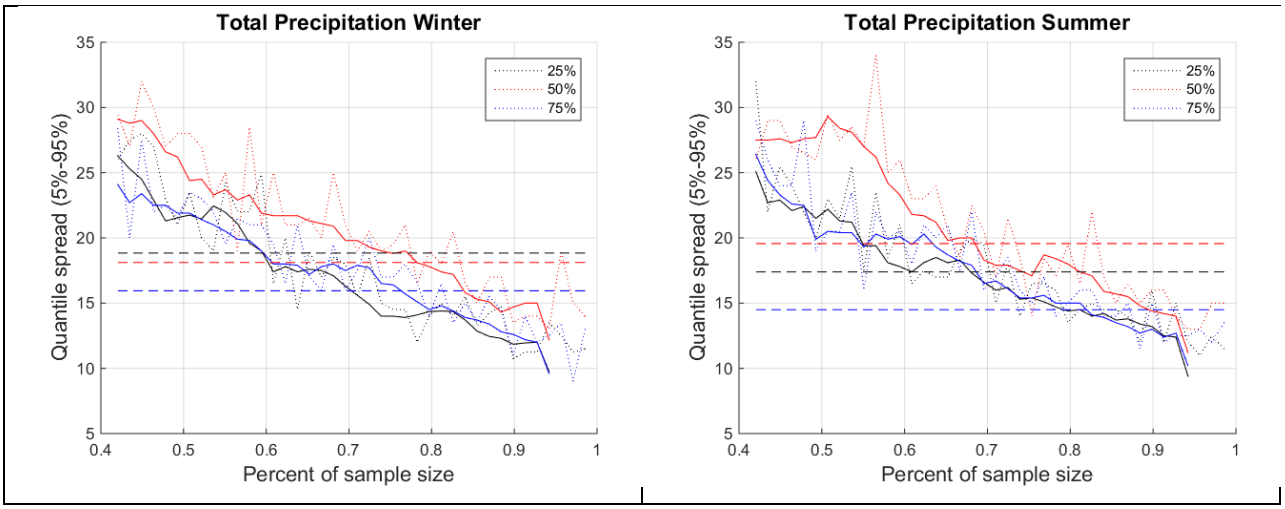

Figure 5.3: The spread between the 5 and 95 percentiles confidence intervals at the 25, 50 and 75 percentiles of the observed CDF (black, red and blue, respectively) as a function of the sample size of the record. The solid lines are moving averages of CI values (dotted lines). The dashed horizontal lines are the estimated spread from the WG simulated ensemble.

In general, it can be said that the winter and summer in Figure 5.2 exhibit a fairly similar pattern. The spread of the simulated 25%, 50% and 75% in both seasons is in between 15-20% (dashed line crossing of the y-axes). These spreads are equivalent to CI that is associated with a sample size that represents 60-80% of the entire observed record (dashed horizontal lines crossing of the observed CI). In summary, it can be stated that the generated span of the ensemble when evaluated for the total season precipitation represents uncertainty in the observed that is associated to a record that is representative of about 60-80% of the years.

Cited References

Bonta, J.V and R.A. Rao. 1988. Factors affecting the identification of independent storm events. Journal of Hydrology 98:275-293.

Eagleson P.E. Climate, soil, and vegetation. 2. The distribution of annual precipitation derived from observed storm sequences. Water Resources Research 14:(5)713-721.

Eden, S., S.B. Megdal, E. Shamir, K. Chief, and E. Mott Lacroix. 2016. Opening the Black Box: Using a Hydrological Model to Link Stakeholder Engagement with Groundwater Management. Water 8(5), 216 doi:10.3390/w8050216. http://www.mdpi.com/2073-4441/8/5/216

Istok, J.D., S.W. Childs, L. Boersma. 1983. Criteria for defining hydrologic events for use in modeling the response of small agricultural watersheds. Paper Presented at the 1983 Winter Meeting, Am. Soc. Agric. Eng. Pap: 83-2510 33p.

Liu, T. A.Y. Sun, K. Nelson, W.E. Hipke. Cloud computing for integrated stochastic groundwater uncertainty analysis Int. J. Digit. Earth, 2012 (2012), pp. 1-25

Nelson, K. 2010. Risk Analysis of Pumping Impacts on Simulated Groundwater Flow in the Santa Cruz Active Management Area. Keith Nelson. Modeling Report No. 21 http://www.azwater.gov/azdwr/Hydrology/Modeling/documents/Modeling_Report_21.pdf

Restrepo-Posada, P. J., and P. S. Eagleson, 1982. Identification of independent rainstorms. J. Hydrol., 55, 303-319.

Rodriguez-Iturbe, I., Cox, D. R. & Isham, V. (1987), Some models for rainfall based on stochastic point processes, Proceedings of The Royal Society of London, Series A410 , 269–288.

Rodriguez-Iturbe, I., Cox, D. R. & Isham, V. (1988), A point process model for rainfall: further developments, Proceedings of The Royal Society of London, Series A417

Shamir, E. 2017. The value and skill of seasonal forecasts for water resources management in the Upper Santa Cruz River basin, southern Arizona. Journal of Arid Environments. 137: 35-45.

Shamir, E. Megdal, S. Carrillo, C. Castro, LC. Chang, H-I. Chief, K. Corkhill, EF. Eden, S. Georgakakos, PK. Nelson, MK. and Prietto, J. 2015. Climate change and water resources management in the Upper Santa Cruz River, Arizona. Journal of Hydrology. 521: 18-33. https://doi.org/10.1016/j.jhydrol.2014.11.062

Shamir, E., 2014. Modification and Calibration of the Hydrologic Modeling Framework for the Santa Cruz River Basin, Arizona. HRC Technical Note No.71. Hydrologic Research Center, San Diego, CA, http://www.hrc-lab.org/projects/projectpdfs/HRCTN71_20140901.pdf

Shamir E., NE. Graham, J Wang, DM Meko, and KP Georgakakos. Stochastic streamflow scenarios for the Santa-Cruz River at the Nogales gauge, Prepared for the Arizona Department of Water Resources, Santa Cruz, AMA, Hydrologic Research Center Technical Report No. 4, December 2005. http://www.hrc-lab.org/projects/dsp_projectSubPage.php?subpage=santacruz

Shamir, E., Wang, J., Georgakakos, K.P., 2007a. Probabilistic streamflow generation model for data sparse arid watersheds, J. Amer. Wat. Resour. Assoc. 43(5) 1142-1154.

Shamir, E., Graham, N.E. Meko, D.M. Georgakakos, K.P., 2007b. Hydrologic model for water resources planning in Santa-Cruz River, Southern Arizona, J. Amer. Wat. Resour. Assoc. 43(5) 1155-1170.